Supporting information

Dynamically Controlled Growth of Cu-Mo-O Composite Nanosheets for Efficient Electrocatalytic Hydrogen Evolution

Aili Wang[a,b], Lili Zhao[b], Hui Liu[b], Ziqian Zhou[b], Chengbo Li[a], Yong Xiang [a], Weijia Zhou[b*], Feng Hao[a*]

[a] School of Materials and Energy, University of Electronic Science and Technology, Chengdu, 610054, P. R. China

[b] Guangzhou Key Laboratory for Surface Chemistry of Energy Materials, New Energy Research Institute, School of Environment and Energy, South China University of Technology, Guangzhou Higher Education Mega Center, Guangzhou, 510006, China

*Corresponding author. E-mail:

eszhouwj@scut.edu.cn (W. Zhou); haofeng@uestc.edu.cn (F. Hao)

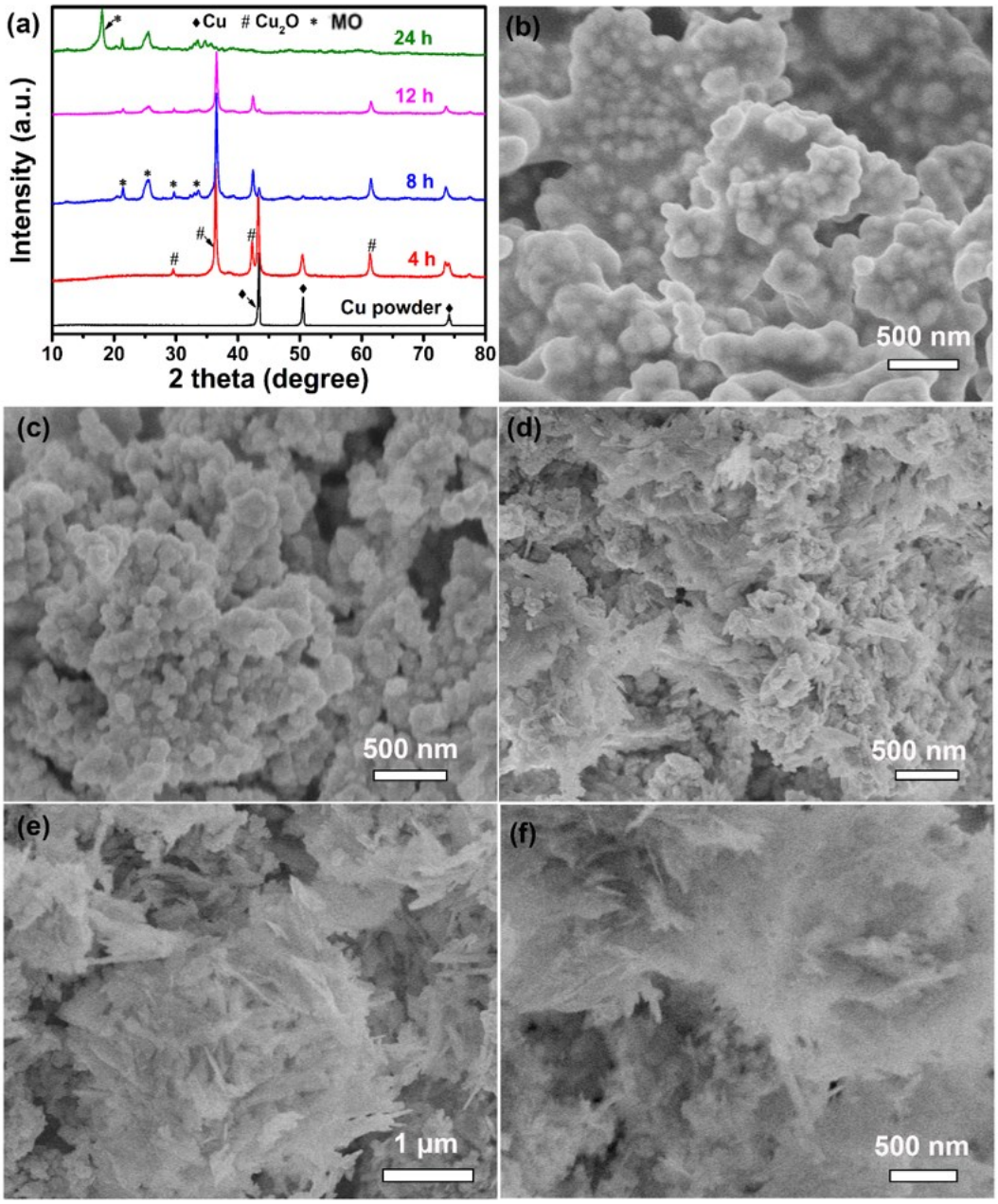

Fig. S1 (a) XRD patterns of Cu powder reacted with $(NH_4)_6Mo_7O_{24}$ solution directly under stirring for 4 h, 8 h, 12 h, and 24 h; SEM images of Cu powder (b) and Cu powder reacted with $(NH_4)_6Mo_7O_{24}$ solution directly under stirring for 4 h (c), 8 h (d), 12 h (e), and 24 h (f).

Firstly, the perfect crystallization of metallic Cu with characteristic peaks (2θ) at 43.3°, 50.4° and 74.1° (PDF#. 04-0836). After the reaction for 4 h, the intensity of diffraction peaks of Cu decreased, but remained the main diffraction peaks and some new peaks at 29.6°, 36.4°, 42.3°, and 61.3° were ascribed to the (110), (111), (200) and (220) planes of cuprite Cu_2O (PDF#. 05-0667). With the reaction time increased to 8 h, the intensity of Cu peaks was weaken further and new peaks of 12.6°, 21.3°, 25.3°, 33.4°, 35.6°, 39.2°, 43.1° and 48.2° were consistent with (020), (-101), (031), (-141), (-112), (211), (-202) and (170) crystal face (PDF#. 36-0405), implying the formation of lindgrenite MO phase. After reaction for 24 h, the diffraction peak of Cu_2O and Cu were disappeared and new peaks at 17.8°, consistent with (011) crystal face of MO (PDF#. 36-0405). Therefore, the successful synthesis of CMO/CF in the presence of Cu_2O was due to excessive Cu on CF substrate. In addition, with the reaction time increasing, the morphology of the product changed as shown in **Fig. S1b-f**, and nanosheets which were appeared at the reaction for 8 h became more and more.

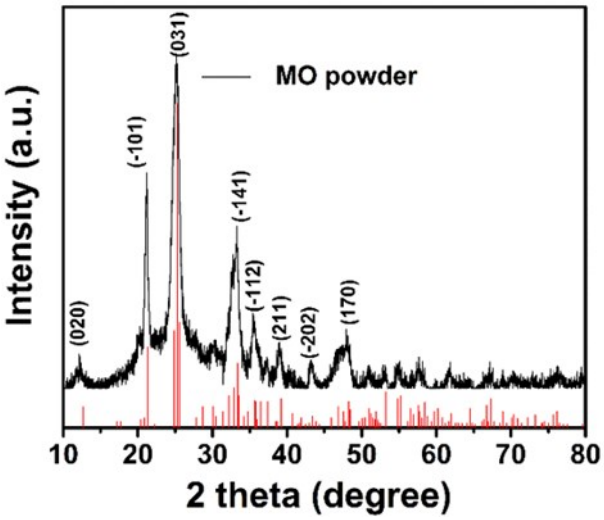

Fig. S2 MO precipitate obtained through Cu NWs/CF reacted with $(NH_4)_6Mo_7O_{24}$ solution under stirring condition.

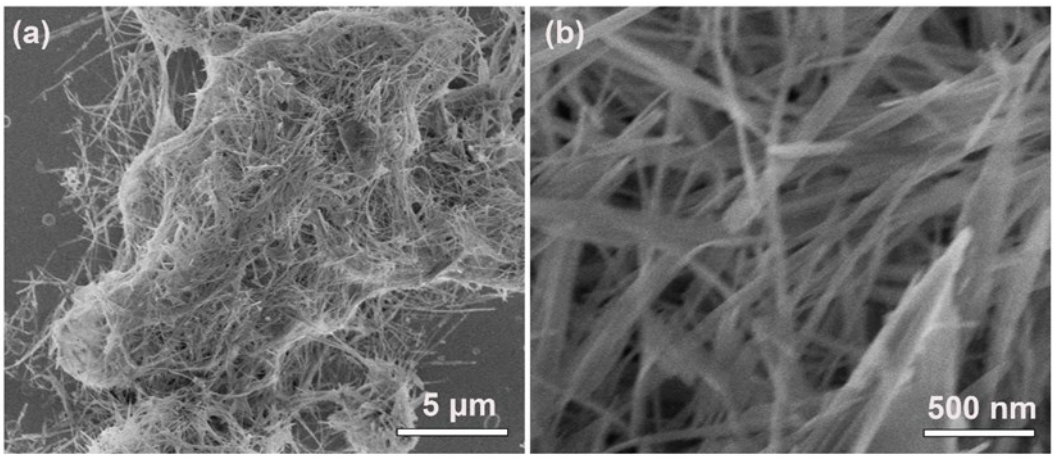

Fig. S3 SEM images of MO powders (precipitation from the reaction of Cu NWs/CF and $(NH_4)_6Mo_7O_{24}$ solution under stirring condition).

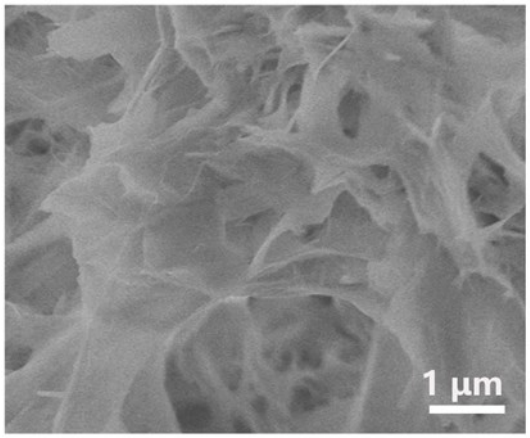

Fig. S4 SEM images of CMOS/CF (CF reacted with $(NH_4)_6Mo_7O_{24}$ solution directly under stirring condition).

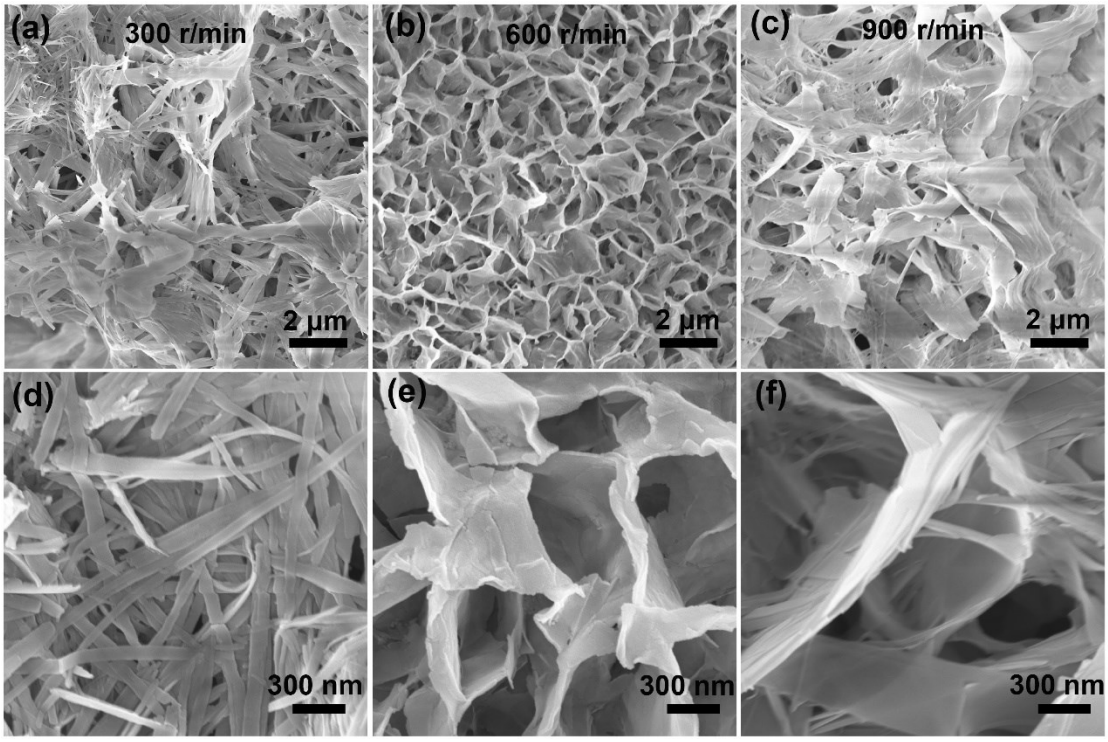

Fig. S5 SEM images of CMOS/CF under different stirring rate of (a, d) 300, (b, e) 600 and (c, f) 900 r/min.

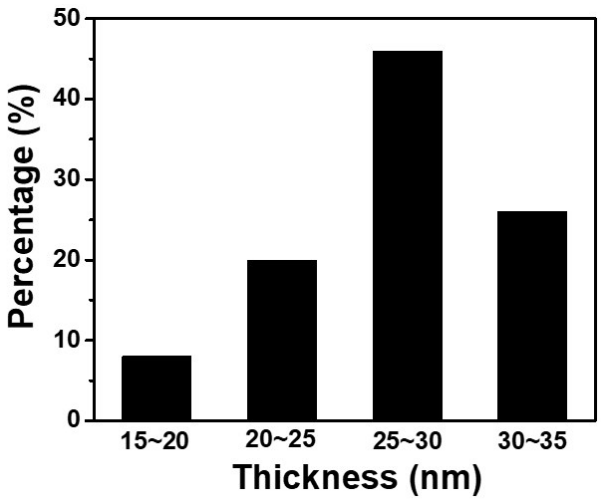

Fig. S6 The thickness distribution of CMOS nanosheet under 600 r/min in 50 points.

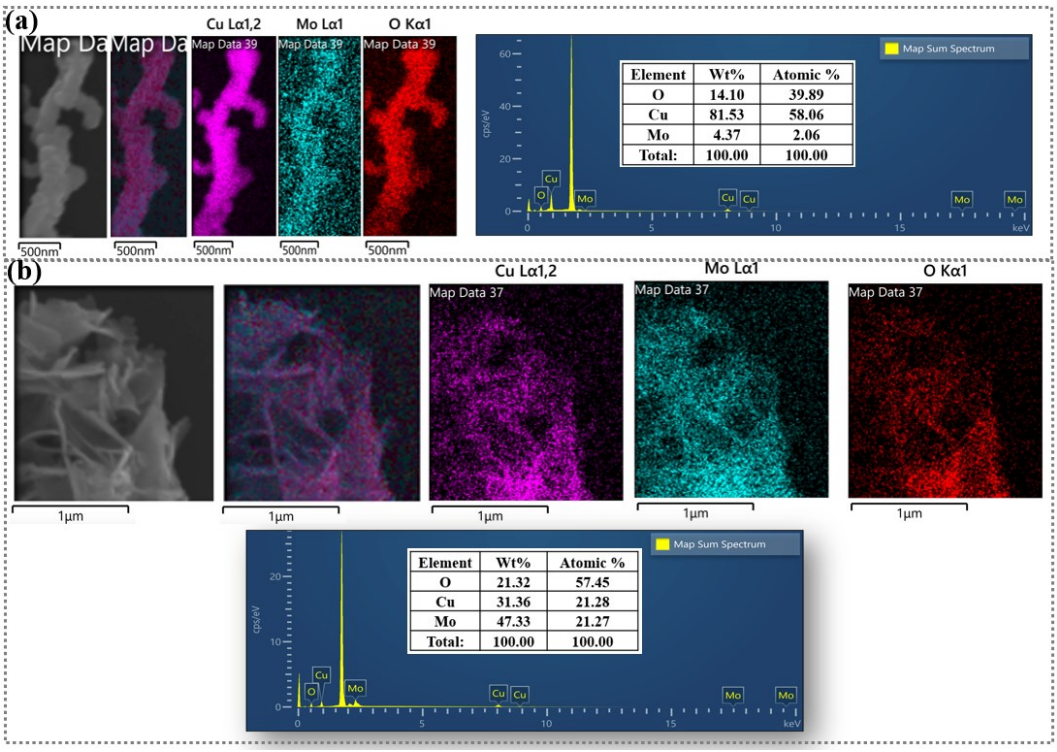

Fig. S7 Energy dispersive spectrometer of CMOW (a) and CMOS (b) scratched from CMOW/CF and CMOS/CF.

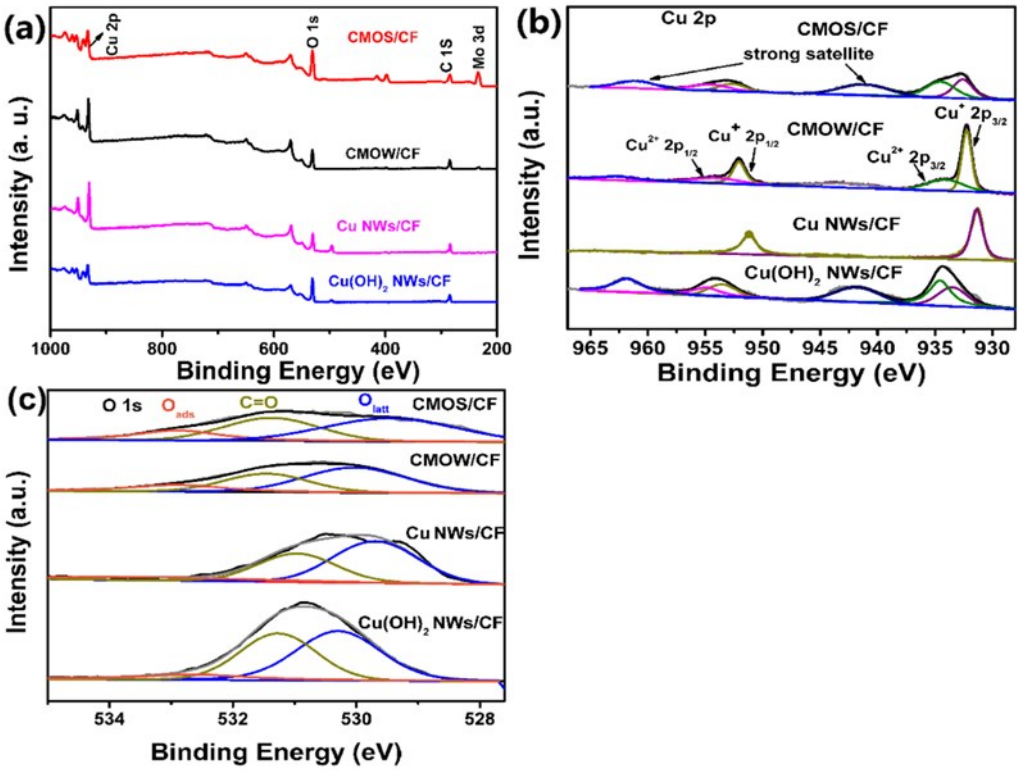

Fig. S8 XPS survey spectra (a) and high-resolution XPS spectra of the Cu 2p (b), O and 1s (c) of $Cu(OH)_2$ NWs/CF, Cu NWs/CF, CMOW/CF and CMOS/CF.

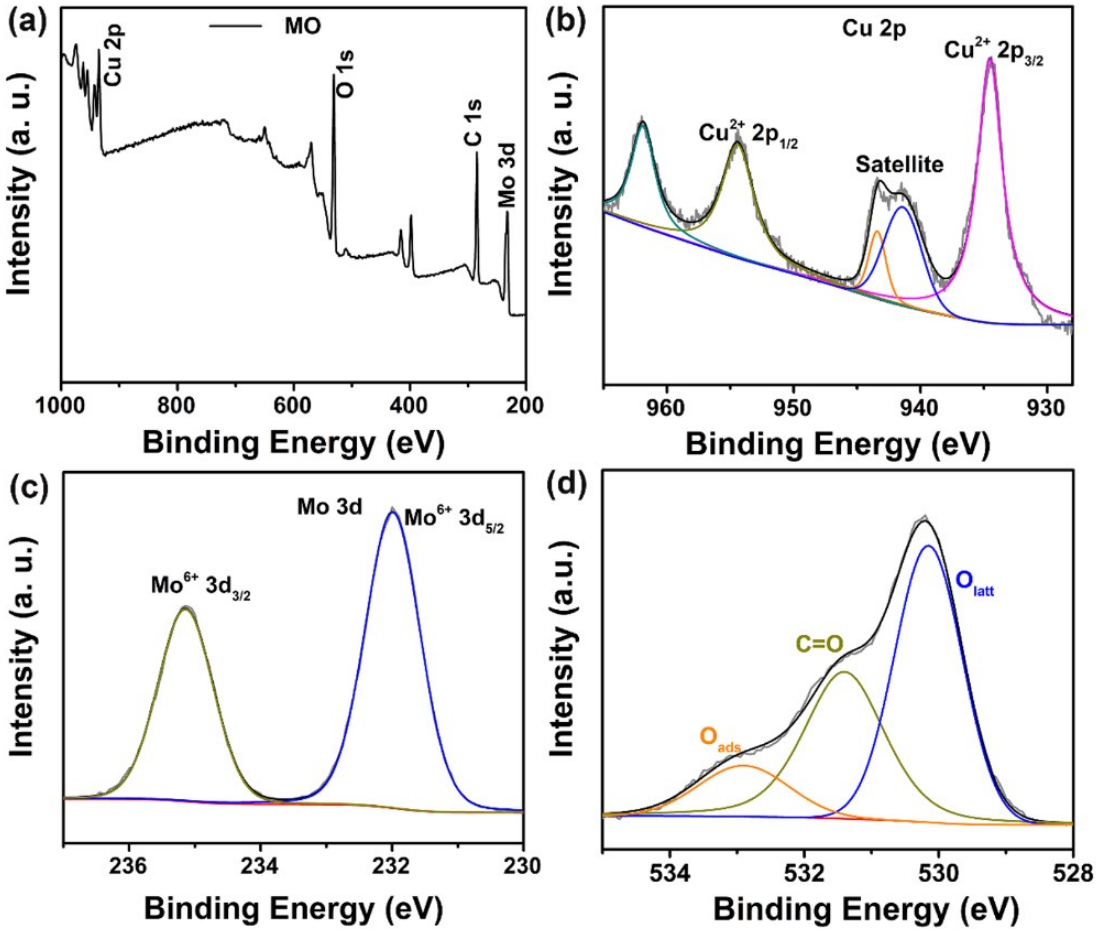

Fig. S9 XPS survey spectra (a) and high-resolution XPS spectra of the Cu 2p (b), Mo 3d (c) and O 2p (d) of MO precipitate powder from the reaction of Cu NWs/CF and $(NH_4)_6Mo_7O_{24}$ under stirring condition.

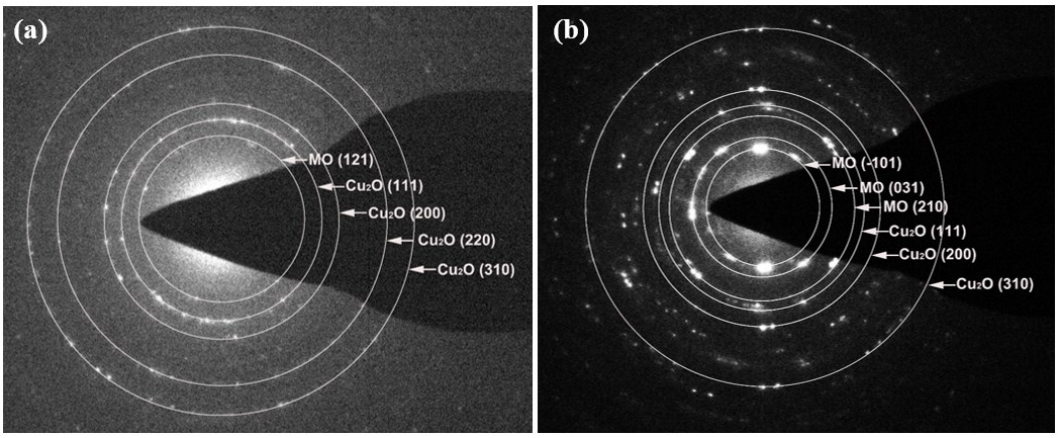

Fig. S10 Selected area electron diffraction patterns of CMOW (a) and CMOS (b).

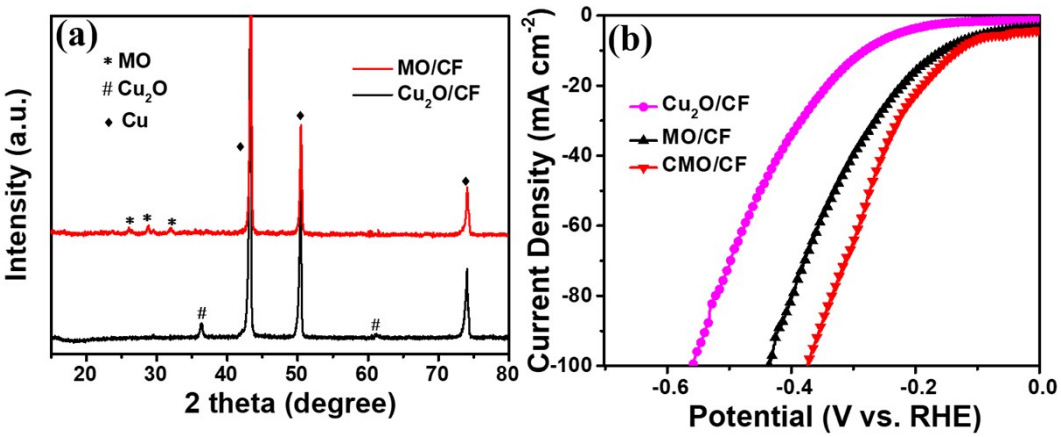

Fig. S11 XRD patterns (a) and polarization curves (b) of MO/CF, Cu_2O/CF and CMO/CF.

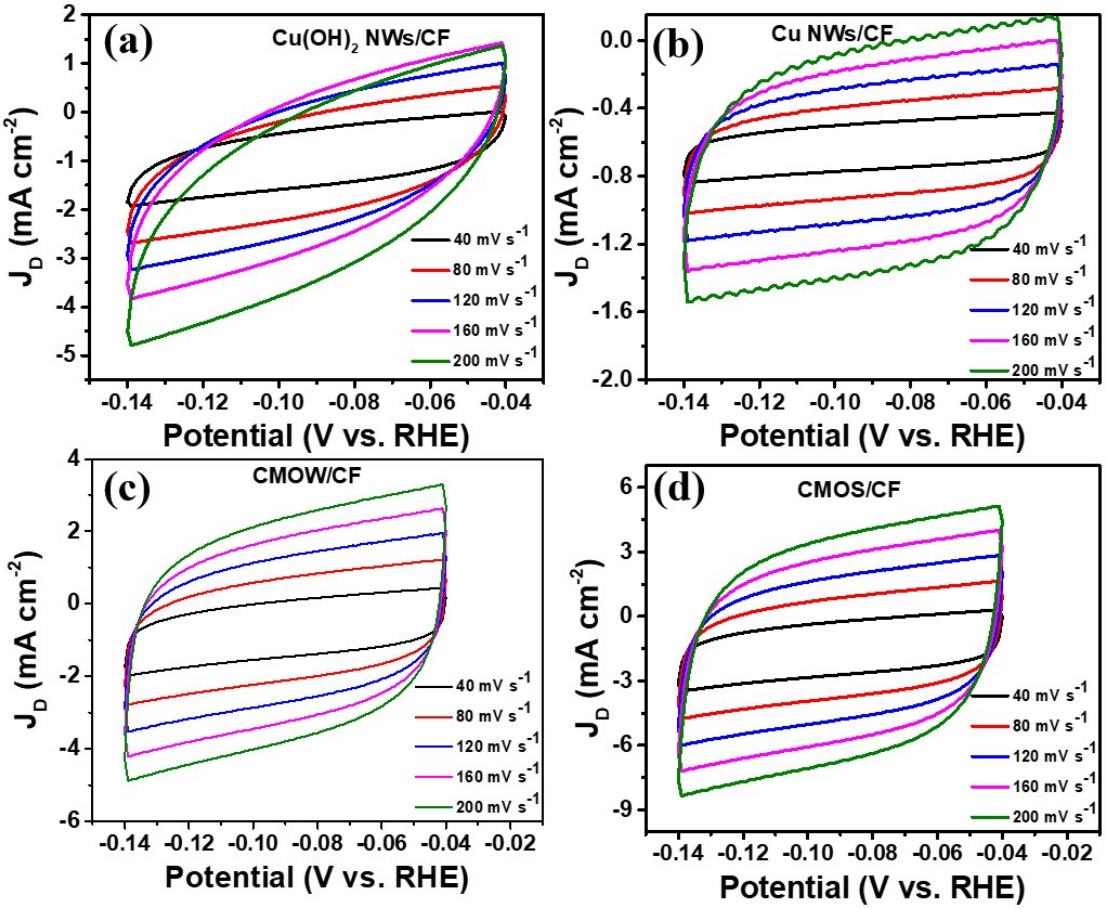

Fig. S12 Linear fitting of the capacitive currents of $Cu(OH)_2$ NWs/CF, Cu NWs/CF, CMOW/CF and CMOS/CF vs scan rates for HER.

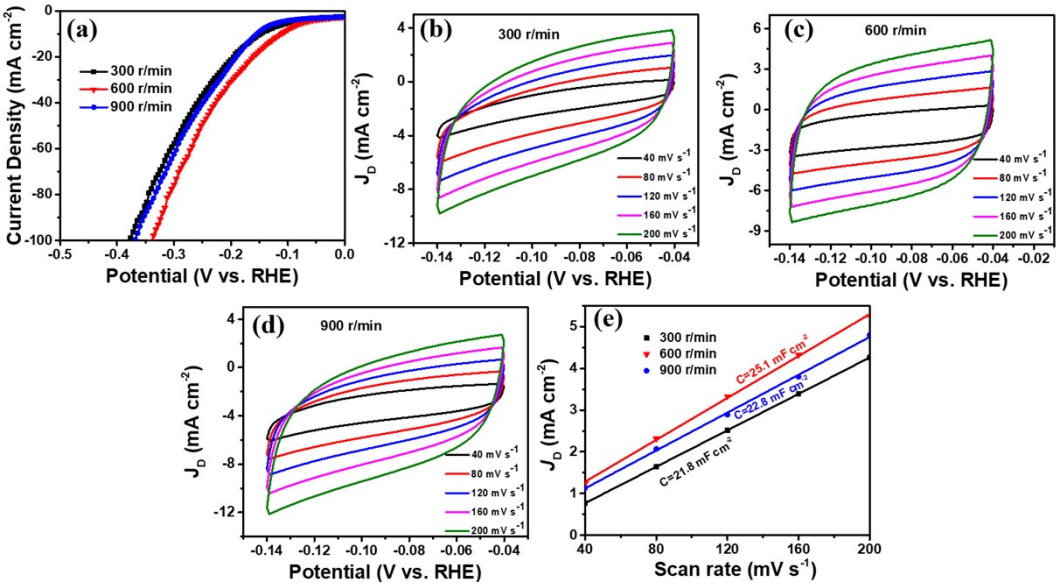

Fig. 13 Polarization curves (a), linear fitting of the capacitive currents vs scan rates (b-d), and the capacitive currents (e) of CMOS/CF under different stirring rate for HER.

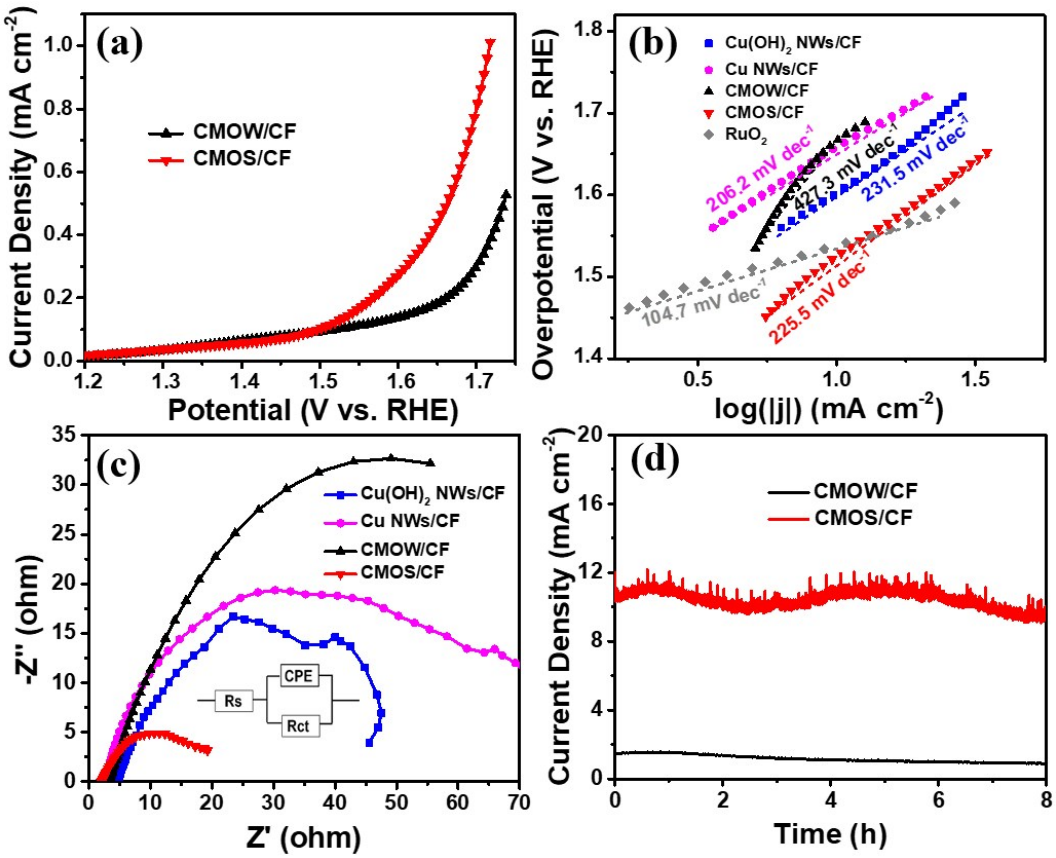

Fig. S14 Polarization curves corrected by electrochemically active area (a), Tafel plots (b), EIS Nyquist plots at 430 mV (c) of $Cu(OH)_2$ NWs/CF, Cu NWs/CF, CMOW/CF, CMOS/CF and (d) current-time plots with an overpotential of 300 mV for OER in 1 M KOH.

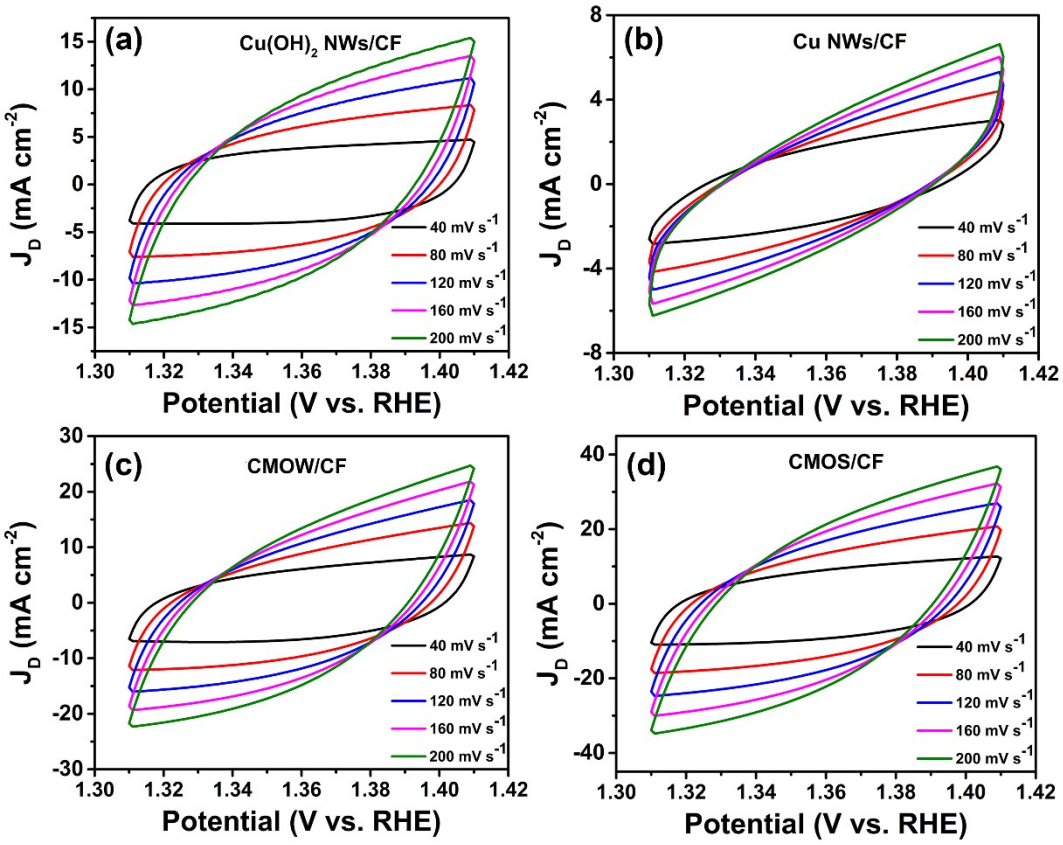

Fig. S15 Linear fitting of the capacitive currents of $Cu(OH)_2$ NWs/CF, Cu NWs/CF, CMOW/CF and CMOS/CF vs scan rates for OER.

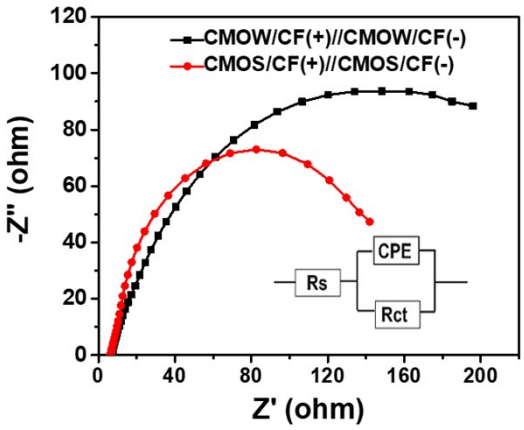

Fig. S16 EIS Nyquist plots of full water splitting at 1.65 V.